UNIVERSITY OF LEEDS

This is a repository copy of *Rates of retrograde metamorphism and their implications for the rheology of the crust: an experimental study*.

White Rose Research Online URL for this paper:
http://eprints.whiterose.ac.uk/80253/

Version: Published Version

Article:
Yardley, BWD, Rhede, D and Heinrich, W (2014) Rates of retrograde metamorphism and their implications for the rheology of the crust: an experimental study. Journal of Petrology, 55 (3). 623 - 641. ISSN 0022-3530

https://doi.org/10.1093/petrology/egu001

Reuse
Unless indicated otherwise, fulltext items are protected by copyright with all rights reserved. The copyright exception in section 29 of the Copyright, Designs and Patents Act 1988 allows the making of a single copy solely for the purpose of non-commercial research or private study within the limits of fair dealing. The publisher or other rights-holder may allow further reproduction and re-use of this version - refer to the White Rose Research Online record for this item. Where records identify the publisher as the copyright holder, users can verify any specific terms of use on the publisher's website.

Takedown
If you consider content in White Rose Research Online to be in breach of UK law, please notify us by emailing eprints@whiterose.ac.uk including the URL of the record and the reason for the withdrawal request.

White Rose university consortium
Universities of Leeds, Sheffield & York

eprints@whiterose.ac.uk
https://eprints.whiterose.ac.uk/

JOURNAL OF PETROLOGY | VOLUME 55 | NUMBER 3 | PAGES 623–641 | 2014 | doi:10.1093/petrology/egu001

Rates of Retrograde Metamorphism and their Implications for the Rheology of the Crust: an Experimental Study

B. W. D. YARDLEY[1,2]*, D. RHEDE[2] AND W. HEINRICH[2]

[1]SCHOOL OF EARTH AND ENVIRONMENT, UNIVERSITY OF LEEDS, LEEDS LS2 9JT, UK

[2]HELMHOLTZ CENTRE POTSDAM, GFZ GERMAN RESEARCH CENTRE FOR GEOSCIENCES, TELEGRAFENBERG, 14473 POTSDAM, GERMANY

RECEIVED MARCH 6, 2013; ACCEPTED DECEMBER 31, 2013
ADVANCE ACCESS PUBLICATION JANUARY 24, 2014

We have carried out experimental studies of the rate at which water is consumed by hydration reactions under mid-crustal conditions. Both pelitic and mafic assemblages are susceptible to extensive hydration in the laboratory on a time scale of weeks to months. Quantitative hydration rate determinations were made using enstatite–oligoclase ± diopside powder mixtures and a natural hypersthene hornfels. Under all conditions, the main hydration product was saponite clay with variable amounts of talc according to the initial proportion of enstatite to plagioclase. The experiments yield consistent rates for water consumption of around 10^{-8} g H_2O per m^2 of mineral surface per second at 400°C and 300 MPa (3 kbar). Additional experiments were run at 300°C and 500°C and at lower pressures (40 MPa), as well as with NaCl; rates appear to be faster at higher temperatures and in the presence of salt, but slower at low pressure. Comparison of powder and core experiments on the natural hornfels indicates that it is primarily the outer surface of the rock core that is available for hydration, with only minor infiltration along grain boundaries. The hydration rates reported here appear to be typical for the types of lithology that demonstrate moderate to high degrees of retrogression along joints and deformation zones in crystalline rocks of the upper crust. Assuming that the surface roughness and damage effects in a natural fault zone are comparable with those of the materials used here in the experiments, the measured hydration rates imply that a natural fracture in crystalline rocks of the middle crust that becomes filled with a water film 0·2 mm in thickness will dry out through incorporation of the water into hydrous phases on a time scale of the order of 10–100 years. This clearly implies that free water has only a short residence time in crystalline rocks of the middle crust or deeper, provided they have cooled below their original temperature of formation and therefore have the potential to undergo retrograde hydration. We infer that the strength of retrograde shear zones in the middle to lower crust will fluctuate through time, with episodes of water infiltration resulting in short periods of water weakening before the water is fully consumed and the rocks become stronger once more.

KEY WORDS: *crustal rheology; hydration rates; hydrothermal experiments; retrogression; saponite*

INTRODUCTION

Retrograde metamorphism is a ubiquitous feature of crystalline rocks, irrespective of the conditions at which they originally formed. Retrogression on a large scale is associated with crustal shear zones. Here, extended water flow has often resulted in metasomatic modification of rock composition as well as hydration. Small-scale retrogression associated with joints and faults along which water has penetrated is much more widespread and occurs in virtually all crystalline rocks. Petrologists investigating high-*T* processes are normally careful to avoid retrograded material near fractures when they collect, but this is unfortunate because retrograde alteration is often the only feature that crystalline rocks preserve from the long period of time between their high-temperature crystallization and their exposure at the surface. As such, it has the potential to provide valuable insights into the long-term state of the

*Corresponding author. Present address: School of Earth and Environment, University of Leeds, Leeds LS2 9JT, UK. Telephone: +44 (0) 113 3435227. Fax: +44 (0) 113 3435259. E-mail: b.w.d.yardley@leeds.ac.uk

© The Author 2014. Published by Oxford University Press. All rights reserved. For Permissions, please e-mail: journals.permissions@oup.com

Downloaded from http://petrology.oxfordjournals.org/ at Edward Boyle Library on August 15, 2014

middle to lower crystalline crust over large parts of the continents away from zones of active prograde metamorphism. This study was intended to improve our understanding of retrogression, and in particular its role as a marker of crustal fluid processes.

Although it is true that retrograde alteration assemblages are indicative of lower temperatures and/or pressures of crystallization than the peak temperature assemblages in a crystalline rock, their most distinctive feature is that they almost invariably involve hydration (Schwartz & Todd, 1941). It was already recognized by Billings (1937) that high-grade metamorphic rocks are unlikely to retain sufficient water to bring about their own subsequent retrogression, so that this is dependent on the infiltration of water from an external source during the cooling history. If it is accepted that retrogression is dependent on infiltrated fluid, then this raises an important question: is retrograde metamorphism developed only locally and incompletely because the hydration reactions are fundamentally slow, even when water has been introduced, or are the hydration reactions themselves rather fast so that the distribution of retrograde features provides a map of where water has infiltrated? Although this question has been debated for many years (Turner, 1968), it has been studied more rigorously in recent years with investigations of hydration in eclogites (e.g. Zack *et al.*, 2001) and has acquired a new urgency in the light of developments in our understanding of crustal rheology.

Water and rheology

Water plays an important role in determining the strength of minerals and rocks, and a role for water is an integral part of models of lithospheric rheology (e.g. Kohlstedt *et al.*, 1995; Blanpied *et al.*, 1998; Burov, 2011). Progressive heating of hydrous materials results in continuous release of water so that initially hydrous rocks normally contain free water throughout prograde metamorphism. In contrast, as soon as crystalline rocks begin to cool free water is consumed by retrograde hydration reactions (Yardley, 2009). The emphasis here is on how quickly this happens and the resulting implications for deformation of cooled crystalline crust.

Water weakening works through both enhanced intracrystalline diffusion creep and by the operation of other deformation mechanisms, notably pressure solution, which are possible only in the presence of free water (Rutter, 1983; Bos & Spiers, 2002). As a result it appears that the strength of wet polymineralic rocks is significantly lower than would be predicted from mineral behaviour alone, even for fine-grained rocks (Kenis *et al.*, 2005). The presence of water as a free phase, rather than just the presence of hydrous minerals, is needed to reduce rock strength to the lowest possible levels. If hydration reactions proceed rapidly then the preservation of high-grade assemblages will imply that the crust is normally dry, with the overall rate of retrogression constrained solely by the supply of water from external sources, whereas if they are slow, then cooled deep crust may contain a free water phase over extended periods of time. Which of these cases prevails will dictate whether the crust is generally weak (water normally present) or generally strong (water normally absent).

Retrograde hydration reactions

The most widespread examples of retrograde hydration reactions include the replacement of hornblende by chlorite and/or actinolite, the replacement of garnet and biotite by chlorite, replacement of Al-silicate polymorphs by sericite, replacement of plagioclase by sericite or epidote, replacement of olivine by serpentine, replacement of enstatite by talc, replacement of omphacite by amphibole and albite in eclogites, and more generally the replacement of basaltic rocks by chlorite, actinolite and epidote. At low temperatures, smectite and other clays dominate reaction products, and carbonation may be important. Because they are a response to infiltration of fluid from an external source, retrograde reactions normally take place far from equilibrium, and it is commonly the case that retrograde assemblages record only a very brief part of the range of temperatures through which a rock has cooled from its original crystallization. Once water is introduced into a crystalline rock under conditions where it will tend to hydrate, it is the rate of the water-saturated hydration reaction that determines how long water persists in the rock, and it is this rate that we have attempted to measure in the laboratory.

Previous experimental studies of rates of retrograde reactions are limited, but Schramke *et al.* (1986) investigated the rate of reaction of andalusite + K-feldspar to muscovite + quartz, and Yardley *et al.* (2010) carried out a study of the rate of hydration of a natural two-pyroxene hornblende granulite, without focusing on a specific reaction. For this study, we made qualitative investigations of several mineral assemblages and carried out detailed measurements of the hydration rate of enstatite-bearing assemblages and a natural two-pyroxene basic hornfels.

EXPERIMENTAL TECHNIQUES

The experiments described here were carried out in conventional cold seal hydrothermal vessels operated at pressures of 400–4000 bars (40–400 MPa) and 300–500°C. The experiments were designed to investigate the products of hydration of mineral mixtures at mid-crustal pressures and measure the amount of water incorporated into secondary hydrous minerals, formed by reaction with mineral particles of known grain size, over times of between 1 week and 20 weeks. In addition, some experiments were carried out using rock cores of a very fine-grained hypersthene hornfels, to investigate the effective surface area

Downloaded from http://petrology.oxfordjournals.org/ at Edward Boyle Library on August 15, 2014

available for hydration in crystalline rocks; powdered hornfels was reacted in the same way as the mineral mixtures to complete the comparisons. Reaction products were characterized as fully as possible by X-ray diffraction (XRD), scanning electron microscopy (SEM) and electron microprobe analysis (EMPA) techniques. The experiments described here differ from most studies of mineral dissolution in that the charges are mineral-dominated, with only a small amount of water (although this was never consumed completely). They contain relatively coarse grains (*c.* 100 μm) to facilitate textural analysis of the run products and their relationship to parent grains. Fluid composition and pH are undefined but will have been determined by mineral–fluid interactions, except for the addition of NaCl in some experiments. Thus these experiments address significantly different issues from mineral dissolution studies of the same phases (Knauss, 1993; Oelkers & Schott, 1995, 2001).

Starting materials

Diopside (Zillertal, Austria), biotite (Telemark, Norway), plagioclase (oligoclase; Ytterby, Sweden) and enstatite (with traces of secondary talc; Telemark, Norway) were all supplied as cleavage fragments by the Museum für Naturkunde, Berlin. Kyanite (Minas Gerais, Brazil) and garnet (Gore Mountain, New York) were supplied by Dan Harlov, as was finely powdered natural quartz. Mineral fragments were boiled in dilute HCl and distilled water, crushed and sieved, except for biotite, which was finely chopped. The 60–100 μm or 100–200 μm fractions were used in the experiments. Mineral compositions are given in Table 1, and an example starting material (enstatite and oligoclase grains) is illustrated in Fig. 1a. The hornfels is a contact metamorphosed basalt from Camasunary, Skye, Scotland (Ferry *et al.*, 1987), provided courtesy of Fran Entwistle, and has a fine-grained (*c.* 100 μm) granoblastic polygonal texture. It is mainly composed of plagioclase, hypersthene and clinoyroxene, with common magnetite, minor ilmenite and traces of biotite. There are traces of alteration of orthopyroxene to talc and clay. The major mineral compositions of this sample are also included in Table 1.

Methods

Powder experiments

Mineral mixtures (typically *c.* 20–40 mg) were accurately weighed into gold capsules and the capsules were then loaded with a precisely weighed amount (typically *c.* 5–9 mg) of double distilled water or salt solution, crimped and welded using a Lampert PUK U3 microwelder to avoid the risk of water loss. Weighings were carried out to 0·1 μg and great care was taken to ensure that quantities of water were known accurately to ±1 μg. Capsules were loaded into cold seal hydrothermal vessels and maintained to within 5°C of the nominal temperature and 2 MPa of the nominal pressure. Most experiments were carried out in duplicate. At the end of the run period, the vessels were quenched with compressed air and the capsules extracted. Capsules were cleaned, dried and weighed, generally weighing a few tens of micrograms more than at the start of the experiment owing to soiling. The capsules were then punctured with a sharp needle under a binocular microscope, taking great care to control the upwelling of water as pressure was released to avoid loss of material by sputtering. The punctured capsules were redried at 105°C and then reweighed, with the difference between the two weighings being taken to be the weight of free water remaining at the end of the run. It is believed that the largest sources of error occurred at this step. The dissolved load of the fluid at the end of the run was sufficient that if water was lost by sputtering, the weight loss was greater than if water was lost by drying alone. Hence the amount of hydration was underestimated. A similar effect resulted if any grains of charge were lost on the tip of the needle. On the other hand, if any water remained caught in the capsule after drying, the amount of hydration could be overestimated. With hindsight, it would have been possible to make more accurate measures of the amount of fluid consumed by reheating the run products after they had first been dried as described above, and measuring the water released as they broke down. Unfortunately, because of the heterogeneous nature of the reacted charge, this would require breaking down all the run products without any opportunity to investigate them further.

Core experiments

A major uncertainty for kinetic experiments is in estimating the reactive surface area available to the fluid phase. As a result it is difficult to relate the area available in powder experiments to the situation prevailing along a water-filled fracture deep in the crust. Yardley *et al.* (2010) took a conservative approach and assumed that a water-filled crack in mid-crustal crystalline rocks would behave as a plane with two surfaces whose increased area through roughness was the same as that assumed for the increased area of powder grains compared with their geometrical areas (i.e. a factor of 10). They assumed no penetration of water into the rock. To test this approach, we carried out a series of experiments using cylinders drilled from the fine-grained mafic hornfels. Experiments using rock cores were prepared and investigated similarly to the powder experiments. Cores were either 3·00 ± 0·05 mm in length and 2·5 ± 0·02 mm in diameter, or 10·00 ± 0·05 mm in length and 4·60 ± 0·02 mm in diameter, and were prepared to fit tightly into the gold tubing.

HYDRATION RESULTS

Powder experiments

Table 2 provides a summary of the experiments that were satisfactorily loaded and completed. A range of systems

Downloaded from http://petrology.oxfordjournals.org/ at Edward Boyle Library on August 15, 2014

Table 1: Average compositions of minerals used as starting materials

	Mineral separates												Hypersthene hornfels					
	Enstatite		Diopside		Garnet		Plagioclase		K-feldspar		Biotite		Orthopyroxene		Clinopyroxene		Plagioclase	
	mean	SD	mean	SD	mean	SD	mean	SD	mean	SD	mean	SD	mean	SD	mean	SD	mean	SD
wt %																		
SiO_2	58·6	1·18	55·0	0·14	40·1	0·16	64·1	0·38	64·7	0·41	33·9	0·22	54·1	0·20	51·7	0·70	51·1	0·53
TiO_2	0·03	0·02	0·01	0·01	0·03	0·01	b.d.		b.d.		3·20	0·17	0·32	0·10	0·56	0·19	0·08	0·05
Al_2O_3	0·43	0·05	b.d.		22·8	0·11	22·0	0·19	18·1	0·15	12·8	0·35	1·24	0·03	2·22	0·55	30·0	0·45
MgO	39·1	1·14	17·4	0·13	11·49	0·1	b.d.		b.d.		1·16	0·12	27·7	0·24	15·7	0·24	0·09	0·06
FeO	2·05	0·09	2·31	0·06	23·2	0·23	0·04	0·02	b.d.		33·2	0·31	14·7	0·13	6·75	0·81	0·63	0·10
MnO	0·02	0·01	0·42	0·07	0·58	0·03	b.d.		b.d.		2·51	0·12	0·49	0·08	0·26	0·04	b.d.	
CaO	0·05	0·02	26·7	0·17	4·19	0·07	3·69	0·16	b.d.		b.d.		1·37	0·15	22·3	0·95	13·6	0·40
SrO	b.d.		0·17	0·03	0·11	0·02	0·18	0·02	0·23	0·02	0·09	0·02	n.d.		n.d.		n.d.	
Na_2O	b.d.		b.d.		b.d.		9·81	0·2	0·51	0·06	0·34	0·11	b.d.		0·34	0·11	3·81	0·24
K_2O	b.d.		b.d.		b.d.		0·35	0·11	16·19	0·13	8·63	0·15	n.d.		b.d.		0·16	0·05
Total	100·3		102·0		102·5		100·2		99·9		96·1		100·0		99·9		99·5	
n	20		20		23		24		8		21		6		9		17	
Mineral formulae																		
O	12		12		12		8		8		22		6		6		8	
Si	3·95		3·95		2·96		2·83		3·00		5·61		1·95		1·92		2·34	
Ti	0·001		0·001		0·001						0·398		0·009		0·016		0·003	
Al	0·034		0·000		1·99		1·15		0·991		2·50		0·053		0·097		1·62	
Mg	3·92		1·86		1·27		0·001				0·287		1·49		0·871		0·006	
Fe	0·116		0·139		1·44		0·002				4·59		0·442		0·210		0·024	
Mn	0·001		0·025		0·036						0·352		0·015		0·008			
Ca	0·003		2·053		0·332		0·175				0·001		0·053		0·885		0·669	
Sr			0·007		0·005		0·005		0·006		0·009		n.d.		n.d.		n.d.	
Na							0·840		0·046		0·110				0·024		0·339	
K							0·020		0·959		1·821						0·010	
Total	8·03		8·04		8·04		5·02		5·01		15·70		4·01		4·03		5·02	

b.d., below detection; n.d., not determined; SD, standard deviation; *n*, number of points averaged.

were investigated in outline, with qualitative observations of reaction products, whereas quantitative measurements of hydration rates were made on a series of powder assemblages containing orthopyroxene.

Qualitative observations

The experiments summarized in Table 2 include a number of long-duration runs that did not yield quantitative measures of hydration rate but resulted in extensive visible reaction in a range of assemblages. Where reaction was reasonably extensive it was notable that the charge, loaded as a fine powder, had agglomerated during the course of the experiment and was weakly held together in clumps by a matrix of secondary phases when the capsule was open. These agglomerated particles were often sufficiently robust to survive extraction and some examples from a range of assemblages are illustrated below.

Kyanite–biotite–quartz. Experiments were carried out at 300–500°C to try to simulate the retrograde replacement of kyanite by white mica 'shimmer aggregate' (see Yardley *et al.*, 1990, pp. 22 and 30), coupled to chloritization of biotite, and all showed the development of secondary sheet silicates around kyanite grains (Fig. 1b and c). The most extensive alteration was seen at 500°C (i.e. closest to the conditions where the starting assemblage is stable), suggesting that the effect of temperature on mineral reaction rates (which is greater at high T) dominated over the effects of differences in ΔG (greater at low T) in determining the extent of reaction. Reaction products were also coarser

Downloaded from http://petrology.oxfordjournals.org/ at Edward Boyle Library on August 15, 2014

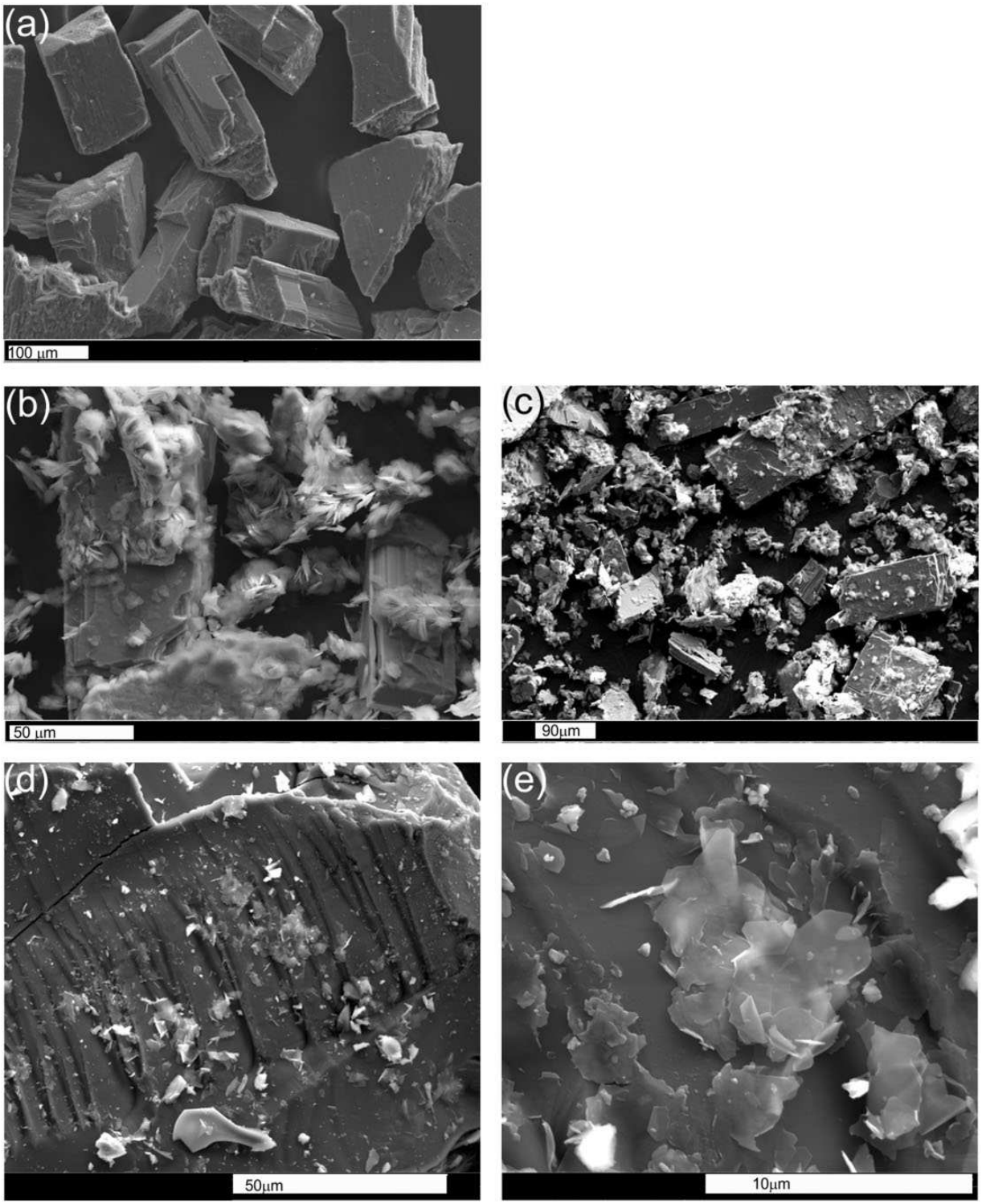

Fig. 1. SEM images of powder materials from qualitative experiments. Details of run conditions and duration are given in Table 2. (a) Enstatite–plagioclase starting material; (b) kyanite fragments coated in clumps of new-grown phengite (see Fig. 2a), capsule 7; (c) run products from capsule 7, showing partially coated kyanite grains and dislodged clumps of phengite; (d) garnet surface showing traces of sheet silicate growth, capsule 10; (e) detail of capsule 10 showing thin platelets of a sheet silicate growing from the garnet surface.

Downloaded from http://petrology.oxfordjournals.org/ at Edward Boyle Library on August 15, 2014

Table 2: Summary of experimental runs using mineral or rock powders as starting materials

Mineral mass												Hydration rate	
Run no.	en (mg)	olig (mg)	qz (mg)		Fluid	Size (μm)	H_2O initial (mg)	*P* (MPa)	*T* (°C)	Duration (h)	H_2O consumed (mg)	H_2O loss/area en + olig (g $s^{-1}m^{-2}$)	Secondary phases [major (trace)]
Enstatite–oligoclase–quartz													
23	4·91	18·51	4·23		H_2O	100–200	4·8234	300	400	664	0·1399	1·28809E – 08	sap (tc) (chl?)
24	19·59	5·25	3·83		H_2O	100–200	6·5415	300	400	592	0·1730	1·87835E – 08	sap tc
25	20·04	7·03	4·00		H_2O	100–200	6·1690	300	400	334	0·2441	4·26956E – 08	sap tc
31	3·58	15·72	3·05		H_2O	100–200	4·1942	300	400	334	0·1115	2·46678E – 08	sap (tc)
32	16·86	12·68	12·26		H_2O	100–200	6·3274	300	400	1368	0·4158	1·57507E – 08	sap tc
35	7·91	16·33	1·74		H_2O	60–100	9·2376	300	400	1368	0·1182	3·03211E – 09	sap (tc) (srp?)
Mean value					H_2O			300	400			1·96351E – 08	
8	20·76	19·27	16·87		H_2O	100–200	6·4947	400	500	1848	5·9857	1·22608E – 07	sap
43	6·95	20·27	1·65		H_2O	60–100	7·4579	40	400	1176	0·0017	4·46041E – 11	sap tc
58	9·97	10·58	2·78		1M NaCl	60–100	6·7819	300	400	672	1·1669	7·40289E – 08	sap tc
Diopside-bearing assemblages													
	en	olig	qz	di									
60	7·18	8·91	3·21	10·88	H_2O	60–100	7·7440	300	400	720	0·3621	2·71849E – 08	sap (tc)
	en	di	qz										
20	16·83	16·30	5·94		H_2O	100–200	5·9409	300	300	3696	5·4481	7·63651E – 08	tc
17	22·64	28·13	7·06		H_2O	100–200	4·7560	300	400	3696	4·3356	3·98061E – 08	tc
14	20·04	23·38	6·97		H_2O	100–200	7·1118	400	500	1848	2·7494	5·89757E – 08	tc
Hypersthene hornfels													
71	24·10				H_2O	60–100	5·9114	100	400	672	0·5488	3·23328E – 08	sap (tc)
72	26·62				H_2O	60–100	6·4378	100	400	1344	0·0208	5·63757E – 10	sap
74	21·54				H_2O	60–100	2·0147	300	400	1272	0·3753	1·32826E – 08	sap
75	20·23				H_2O	>100	5·0509	300	400	1272	0·2611	1·69111E – 08	sap
Qualitative experiments													
Biotite–kyanite–quartz													
	bio	ky	qz										
5	15·56	8·93	8·67		H_2O		5·8287	3000	300	3696			ph
6	25·46	10·15	5·08		H_2O		6·1707	3000	400	3696			ph
7	22·26	9·66	5·86		H_2O		6·7965	4000	500	1848			ph (chl)
Garnet–quartz													
	gt	qz											
10	21·48	8·78			H_2O		6·0573	4000	500	1848			(sheet silicate)

en, enstatite; di, diopside; olig, oligoclase; qz, quartz; bio, biotite; ky, kyanite; gt, garnet; sap, saponite; tc, talc; chl, chlorite; srp, serpentine; ph, 'phengitic mica'.

grained in the higher temperature experiments. Semi-quantitative energy-dispersive spectrometry (EDS)–SEM analysis of the sheet silicates around kyanite indicates that they are phengite. Although much of the biotite remains fresh, it has sometimes developed overgrowths that yield a low-K spectrum identified as chlorite.

Garnet–quartz. Secondary alteration products were not obvious in experiments with only garnet and quartz, but Fig. 1d and e shows a garnet surface from an experiment at 400 MPa and 500°C exhibiting some development of platelets of phyllosilicate, mainly edge on to the garnet surface (Fig. 1e). Although these plates are too small for quantitative analyses, EMPA measurements on a polished block indicate that they are chlorite, as they lack Ca, present in the parent garnet, and have enhanced levels of Al relative to Si. The extent of reaction is clearly limited, as

Downloaded from http://petrology.oxfordjournals.org/ at Edward Boyle Library on August 15, 2014

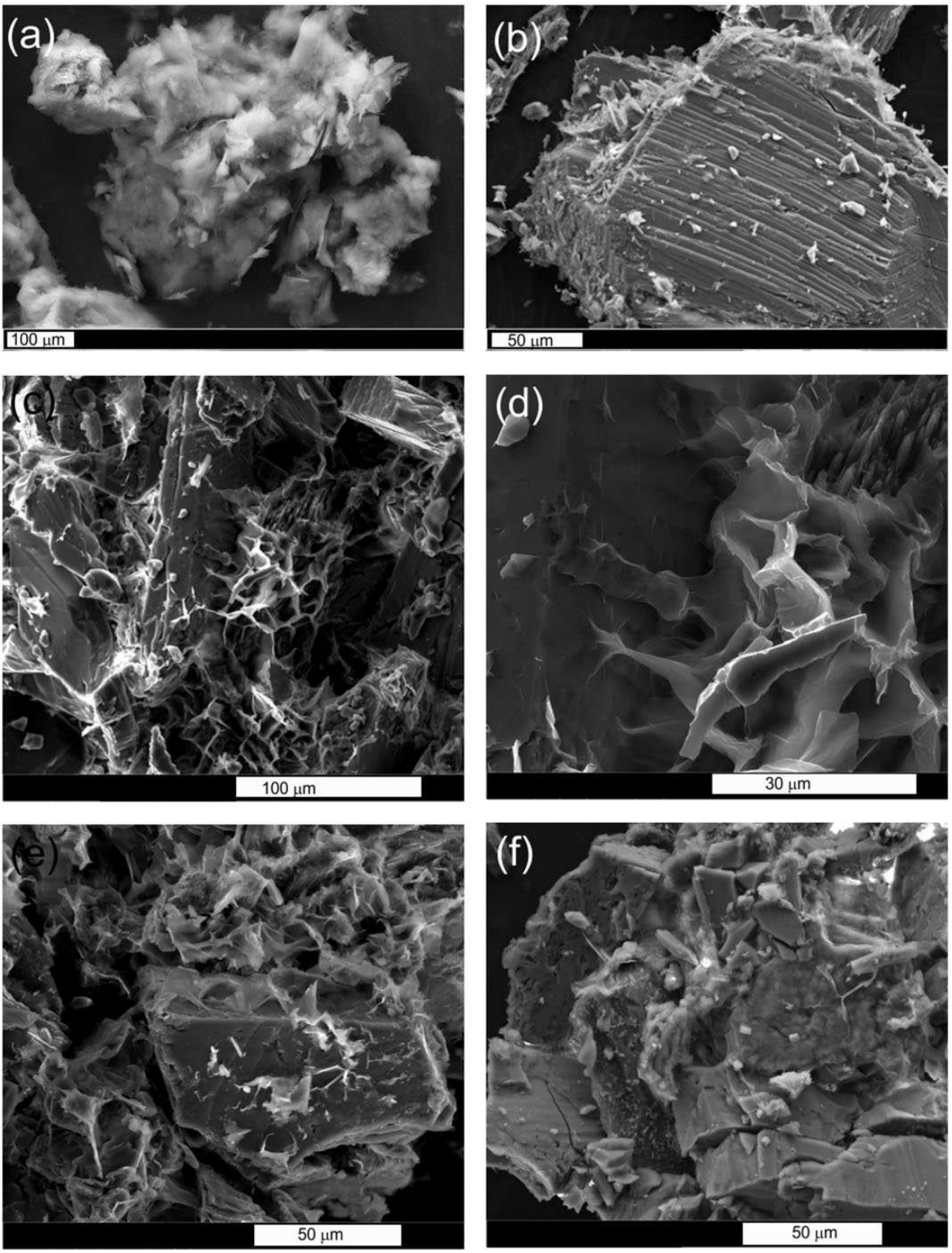

Fig. 2. SEM images of powder materials from quantitative experiments. Details of run conditions and duration are given in Table 2. (a) Secondary talc extensively replacing original enstatite from an enstatite–diopside–quartz experiment, capsule 17; (b) diopside grain from an enstatite–diopside–quartz experiment, showing very little evidence of reaction after 1848 h at 500°C and 400 MPa, capsule 14; (c) original particles of an oligoclase–enstatite charge cemented together by honeycomb-textured saponite, capsule 35; (d) detail of capsule 35 showing a deeply pitted enstatite surface gripped by honeycomb saponite overgrowths; (e) relatively unaltered oligoclase fragment from an oligoclase–enstatite charge in NaCl solution, cemented to enstatite remnants by honeycomb-textured saponite, capsule 57; (f) poorly welded charge from an oligoclase–enstatite experiment at lower pressure (40 MPa), capsule 42.

Downloaded from http://petrology.oxfordjournals.org/ at Edward Boyle Library on August 15, 2014

conchoidal fractures on the garnet surface retain sharp edges (Fig. 1d). Although only limited corrosion of garnet took place in these experiments, Yardley *et al.* (2010) illustrated much more extensive corrosion of garnet reacted with water under similar conditions as part of a natural rock assemblage. This may indicate that garnet reacts more rapidly in a natural multicomponent system than in the simplified garnet–quartz assemblage investigated here.

Enstatite–diopside–quartz. Experiments were carried out in an attempt to produce secondary actinolite from pyroxenes, but failed in this objective. Enstatite shows extensive replacement by talc (Fig. 2a) but diopside does not appear to have reacted to a significant degree (Fig. 2b). None of the experiments in this study produced amphibole as a product, although Yardley *et al.* (2010) documented the development of bundles of secondary actinolite during very similar experiments with hornblende in the starting material. It appears that the immediate hydration products of mafic rocks may be determined by kinetic factors, including the nature of the available substrates for nucleation.

Enstatite–oligoclase quartz. Experiments with enstatite and oligoclase were carried out using both H_2O and H_2O–NaCl fluids (Table 2) and resulted in extensive growth of sheet silicates in most experiments. The main product was a saponite clay, which formed a honeycomb-textured cement loosely bonding the original grains together (Fig. 2c and e). Although oligoclase is involved in the saponite-forming reaction, estatite shows the most obvious replacement textures (Fig. 2d), and is heavily pitted in experiments at 300 MPa. Lower pressure (40 MPa) experiments, also at 400°C, show less extensive pitting of enstatite (Fig. 2f). Saponite also grows from oligoclase surfaces as platy grains grown edge on to the substrate surface. Small amounts of talc were sometimes present.

Enstatite–diopside–oligoclase–quartz. Two experiments were carried out using this assemblage, and results were closely comparable with those with enstatite–oligoclase–quartz, confirming the low reactivity of diopside. Saponite again forms honeycombs cementing the primary grains together, but traces of talc occur also. It is clear that, whereas diopside has no effect on the hydration of enstatite in the presence of quartz, plagioclase is sufficiently reactive to release Al and Ca so that saponite is the main product of enstatite breakdown in place of talc. Details of the reaction are discussed further below.

Hypersthene hornfels. Four experiments with the natural hornfels at 100 and 400 MPa yielded qualitatively similar results to those carried out with mineral mixtures. At the end of the experiments, the powdered charge was loosely held together by a honeycomb of saponite, but there was no evidence of talc. The saponite composition differed in detail from that made with mineral mixtures (see below).

This series of experiments demonstrates that a wide range of common minerals found in crystalline rocks of the mid to lower crust will react readily with water over a time scale of months, generally with significant reaction apparent at temperatures as low as 300°C. There were clear differences in reactivity between phases, with no reaction observed for diopside whereas enstatite was particularly reactive. The textural changes observed are closely comparable with those seen in natural assemblages; for example, kyanite developed mantles of white mica very reminiscent of 'shimmer aggregate' textures commonly encountered in natural kyanite schists, whereas orthopyroxene was replaced by saponite or talc forming pseudomorphs extending along the cleavage directions.

Quantitative measurements of hydration rates

The changes in the weight of water are documented for a range of experiments on orthopyroxene-bearing assemblages in Table 2, together with the masses of the original charges. Many experiments resulted in the consumption of around 100 μg of water, and this is consistent with the observed clay abundance. Four experiments included in Table 2 (run numbers 8, 14, 17 and 20) show suspiciously large weight losses, because there is insufficient solid starting material to account for all the water apparently consumed. These are all experiments with very long run times and significant growth of secondary phases. The results have been retained for most of the subsequent analysis because they provide an effective upper limit to the possible reaction rates and highlight the magnitude of the effects that will be introduced into the interpretation by experimental errors. Capsules 14 and 17 have estimated talc contents near 50 wt % from XRD, suggesting that the measured water consumption is too high by a factor of *c.* 3–5.

Hydration rates were calculated from the measured weight changes, combined with estimated geometric surface areas calculated from the dominant grain sizes in each sieve fraction and multiplied by an arbitrary roughness factor of 10 (from Allan *et al.*, 2011) to compensate for the complexity of the natural surfaces. Surface area calculations are summarized in Table 3. Because diopside showed no evidence of reaction, only the surface areas of enstatite and oligoclase have been included in the rate calculation, except for the experiments with natural hornfels where it was only possible to estimate a total surface area. The error introduced by this uncertainty is significantly smaller than the uncertainty in the total dataset, and so is considered acceptable. We have been unable to measure Brunauer–Emmett–Teller (BET) surface areas because of the small amounts of powders available, but it is likely that they would be significantly greater than those reported here. The effective surface area available to interact with water is discussed below in the context of experiments with cores, but, clearly, it is important to interpret the rates we report using the same assumptions about reactive surface areas as were made in obtaining them.

Downloaded from http://petrology.oxfordjournals.org/ at Edward Boyle Library on August 15, 2014

Table 3: Calculations of surface area for mineral powders used in the experiments

				Single grain				Per gram	
Mineral	Dimensions (μm)			Volume (cm^3)	Area (m^2)	Density	Mass (g)	Area* ($m^2\ g^{-1}$)	Rough area† ($m^2\ g^{-1}$)
enstatite	80	60	60	2·88E – 07	2·64E – 08	3·2	9·22E – 07	2·86E – 02	2·86E – 01
	150	100	100	1·50E – 06	8·00E – 08	3·2	4·80E – 06	1·67E – 02	1·67E – 01
oligoclase	80	60	60	2·88E – 07	2·64E – 08	2·65	7·63E – 07	3·46E – 02	3·46E – 01
	150	100	100	1·50E – 06	8·00E – 08	2·65	3·98E – 06	2·01E – 02	2·01E – 01
diopside	80	60	60	2·88E – 07	2·64E – 08	3·4	9·79E – 07	2·70E – 02	2·70E – 01
	150	100	100	1·50E – 06	8·00E – 08	3·4	5·10E – 06	1·57E – 02	1·57E – 01

*Geometric surface area calculated directly from the estimated dimensions.
†Geometric surface area arbitrarily increased by a factor of 10 to reflect surface roughness.

A detailed series of experiments was performed using enstatite–oligoclase–quartz mixtures in pure water at 400°C and 300 MPa, with a range of run times. Rates were calculated based on the combined surface area of enstatite and oligoclase, as both participate in the saponite-forming reaction. The results for these mixtures are presented in Table 2 and Fig. 3. It is clear from Fig. 3 that, despite significant variation, most experiments duplicate to within a factor of two, and the hydration rate data are scattered over about an order of magnitude, with the exception of an experiment carried out at low pressures (40 MPa), which yielded a much lower rate. This value seems anomalous given the readily visible saponite developed in the charge, but has been retained to indicate an absolute lower limit. The highest rates were measured for the shortest experiments, and could represent anomalously fast reaction of fines in the charge, or slowing down of the reaction owing to mantling of the reactive surfaces by product sheet silicates. Because SEM examination of the starting material did not reveal the presence of significant fines (Fig. 1a), we infer that it is most likely that reaction slowed as surfaces became mantled. However, as the primary purpose of carrying out the measurements was to determine the likely residence time of water in crystalline rocks of the mid-crust, we have preferred the results from the longer duration experiments and deduce a mean hydration rate (i.e. rate of incorporation of water into hydrous mineral lattices) of 2×10^{-8} g H_2O m^{-2} s^{-1} with the experimental uncertainty being a factor of 2·5. This is equivalent to a rate of about 1×10^{-9} mol H_2O m^{-2} s^{-1}. Experiments were also performed at 400°C and 300 MPa with a 1 M NaCl solution, and additional experiments with pure H_2O fluid were performed at 500°C. With NaCl and the same P–T conditions, the hydration rate was about half an order of magnitude higher than for pure H_2O fluids (Fig. 3, Table 2); however, the long duration run at 500°C yielded an improbably high weight loss and the somewhat elevated rate for this experiment is probably an overestimate as noted above.

Quantitative measurements were also made for experiments with enstatite–diopside–oligoclase–quartz and enstatite–diopside–quartz mixtures and are included in Fig. 3. Within error, the rate for the run containing diopside is the same as those determined for enstatite–oligoclase–quartz mixtures. The runs without oligoclase generated talc rather than saponite, and although extensive retrogression is apparent in these long-duration experiments, the rates must be upper limits because the amount of water apparently consumed is more than would be required to completely hydrate the starting materials to talc. Finally, a few runs were carried out using powdered hypersthene hornfels material, from the same sample that was used for the experiments with rock cores. Here it was only possible to estimate a total surface area.

Results of the hornfels experiment are also included in Fig. 3, and it is clear that very similar rates are obtained for a wide range of experiments involving orthopyroxene.

A few experiments gave anomalously low hydration rates, and indeed occasionally the amount of water appeared to increase. The method has the potential for errors that are far larger than simple weighing errors and, based on the amounts of secondary minerals present, we think it likely that the low hydration rate recorded for capsule 42 (40 MPa experiment) is an underestimate. Secondary sheet silicates are clearly present as run products (Fig. 2f), even though the enstatites are less heavily altered than those from higher pressure experiments (Fig. 2). Because of the nature of the method, small uncertainties in the weights of water translate readily into order of magnitude changes in hydration rate, and in this case it is likely that the true hydration rate value is intermediate between that reported here (Table 2) and the mean value from other experiments with the same starting materials (Fig. 3).

Downloaded from http://petrology.oxfordjournals.org/ at Edward Boyle Library on August 15, 2014

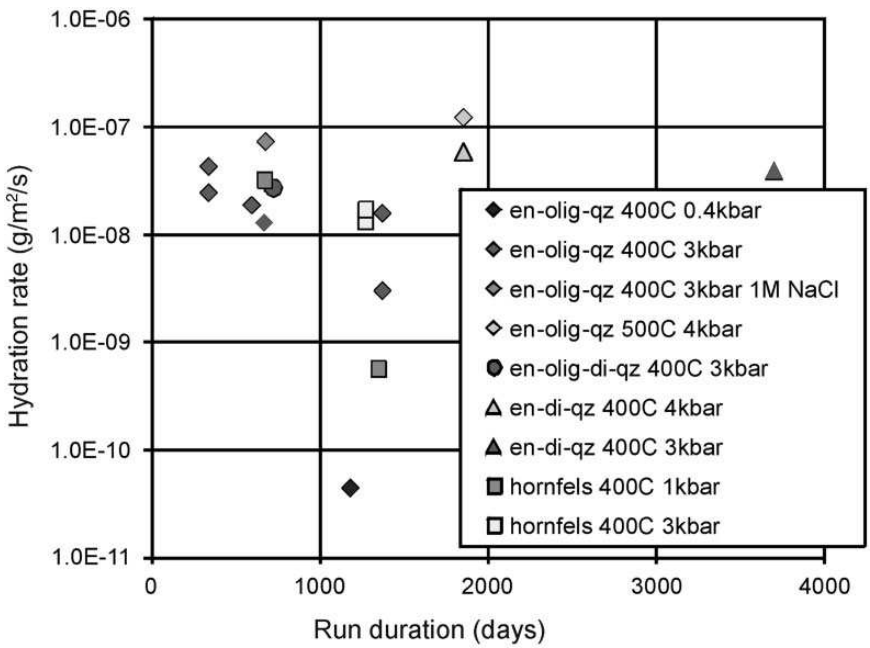

Fig. 3. Experimental hydration rates for all orthopyroxene-bearing experiments, including powdered hornfels (expressed as g H_2O consumed per second per m^2) calculated using geometrical estimates of surface area assuming an arbitrary surface roughness factor of 10, shown as a function of run time. (Note the strong clustering about a rate between 10^{-7} and 10^{-8} g m^{-2} s^{-1}, except for experiments at lower pressures.)

Core experiments and the surface area problem

Experiments were carried out using a similar method to the powder experiments (Table 4). Water consumption owing to hydration of rock cores proved too small to be reliably determined, although new saponite clay can clearly be seen coating the cores (Fig. 4). A conspicuous film of quench silica was also visible on the surface of the cores when the capsules were opened (Fig. 4b and d). Although experiments were carried out at temperatures between 300°C and 500°C, the coating mineral is in all cases saponite, which has grown in a honeycomb texture. There is, however, a significant difference in the size of the crystals with temperature (Fig. 4). The honeycomb cells in the clay structures grown at 300°C are around 2 μm across (Fig. 4a), whereas those formed at 500°C are commonly 30–50 μm across (Fig. 4c). There is no obvious difference in the size of the saponite cells between experiments carried out with pure water and with NaCl solution under the same P–T conditions (Fig. 4b and d).

Back-scattered electron (BSE) imaging of sections of the reacted cores (Fig. 5) show extensive replacement of those orthopyroxene grains that intersect the core surface (Fig. 5b and c). Saponite grains replacing orthopyroxene are of very similar composition to those growing out from the original core surface, although talc may also be present. Orthopyroxene grains within the rock core show very limited alteration along fractures and this is almost certainly original alteration present in the sampled hornfels (Fig. 5a). The observed pattern of alteration demonstrates that, once hydration commences, water penetrates the orthopyroxene grains themselves in preference to the grain boundary network, although minor growth of saponite in plagioclase–plagioclase grain boundaries has been observed. Overall, material is redistributed from the core interior to its surface, so that orthopyroxene dissolution is not notably inhibited by saponite growth. This suggests that the reaction mechanism may involve a decrease in solid volume at the sites of orthopyroxene grains, coupled to precipitation of saponite on the core surfaces. Dissolution was most effective on orthopyroxenes that were initially exposed at the core surface.

Based on reaction at the original core surface area (*c.* $3{\cdot}3 \times 10^{-5}$ m^2) only, with the same assumed roughness as for the grains used for powder experiments, we would expect *c.* 2·5 μg of H_2O to be consumed in an 8 week run at 300 MPa and 400°C, using the mean hydration rate of the powdered hornfels under these conditions from Table 2. Alternatively, based on the images in Fig. 5, we can estimate the amount of water required to hydrate the orthopyroxene in the outer 100 μm of a core, assuming 5 vol. % of the rock was composed of orthopyroxene that became hydrated and 15 mg of H_2O was consumed per 100 mg orthopyroxene hydrated. This calculation yields a value of 5 μg of H_2O consumed, which is in reasonably good agreement with the estimate made from powder

Downloaded from http://petrology.oxfordjournals.org/ at Edward Boyle Library on August 15, 2014

Table 4: Summary of experiments using hypersthene hornfels cores as starting material

Run no.	Wt. core (mg)	H_2O initial (mg)	Fluid	*P* (MPa)	*T* (°C)	Duration (h)	Secondary phases
Small, solid cores							
27	44·44	7·9934	H_2O	300	400	664	sap
29	43·96	5·9792	H_2O	300	400	592	sap
36	45·72	10·4584	H_2O	300	400	334	sap
37	44·22	10·402	H_2O	300	400	1368	sap
39	44·88	8·7904	H_2O	300	500	672	sap
40	44·21	12·842	H_2O	300	400	334	sap
41	44·89	15·0559	H_2O	40	400	1176	sap
50	44·93	41·7061	H_2O	40	400	1176	sap (tc) (chl?)
51	45·49	10·215	H_2O	300	500	672	sap
52	43·67	9·6525	H_2O	300	300	840	sap
53	45·2	8·663	H_2O	300	300	840	sap
55	41·87	7·9347	1·0M NaCl	300	400	840	sap (tc) (chl?)
56	43·82	7·2269	1·0M NaCl	300	400	672	sap
Large, solid cores							
46	506·49	70·56	0·1M NaCl	300	400	1368	sap
47	471·04	101·87	H_2O	300	400	1368	sap
48	491·64	91·69	H_2O	300	400	1368	sap
49	494·66	108	0·1M NaCl	300	400	1368	sap
63	493·02	48·72	0·5M NaCl	100	400	672	sap
65	484·12	44·62	0·5M NaCl	100	400	1368	sap

Abbreviations are as for Table 2.

reaction rates assuming that only the core surface is reactive: internal grain boundaries within the core are not significant. It is perhaps surprising that we did not obtain consistent evidence of incorporation of water into hydrous phases by weighings in these experiments, as water was nominally weighed to better than 1 μg. We suspect that the source of this discrepancy may be the presence of traces of free or loosely bound water in the core when it was weighed dry, owing to insufficiently aggressive drying before loading the capsules. For the larger cores, the greater total weights of rock and water are sufficiently large that weighing errors would swamp the small weight changes.

CHARACTERIZATION OF RUN PRODUCTS AND DETERMINATION OF THE REACTIONS INVESTIGATED

In addition to SEM imaging, run products have been investigated by XRD and, in some cases, EMPA. Not all replicate experiments have been investigated in detail, however. Experiments with powdered hornfels yield an XRD peak close to 6° 2-theta (Cu Kα radiation), which we have assigned to saponite. Saponite is an Mg-rich trioctahedral smectite that is well known to form metastably in mafic compositions at elevated temperatures (Seyfried & Bischoff, 1979). It is also present in the hornfels core experiments. Powder experiments with enstatite and diopside, but without plagioclase, yielded clear peaks for talc, whereas experiments with oligoclase often yielded more complex peaks between 6 and 7° 2-theta, reflecting the greater variability of clay compositions (below), and normally also talc peaks. It is not possible to identify any systematic differences between saponite from experiments run under different *P*–*T* conditions from the XRD traces, and this was investigated further by EPMA.

Small clumps of run products from the powder experiments (original grains loosely cemented by secondary sheet silicates) were mounted in epoxy and polished for EPMA. It was generally very difficult to obtain a good polish, both because the clays are very soft and because it was difficult for the resin to adequately impregnate the honeycomb texture (Fig. 2), and as a result most analyses give anomalously low totals. Analysis was carried out at

Downloaded from http://petrology.oxfordjournals.org/ at Edward Boyle Library on August 15, 2014

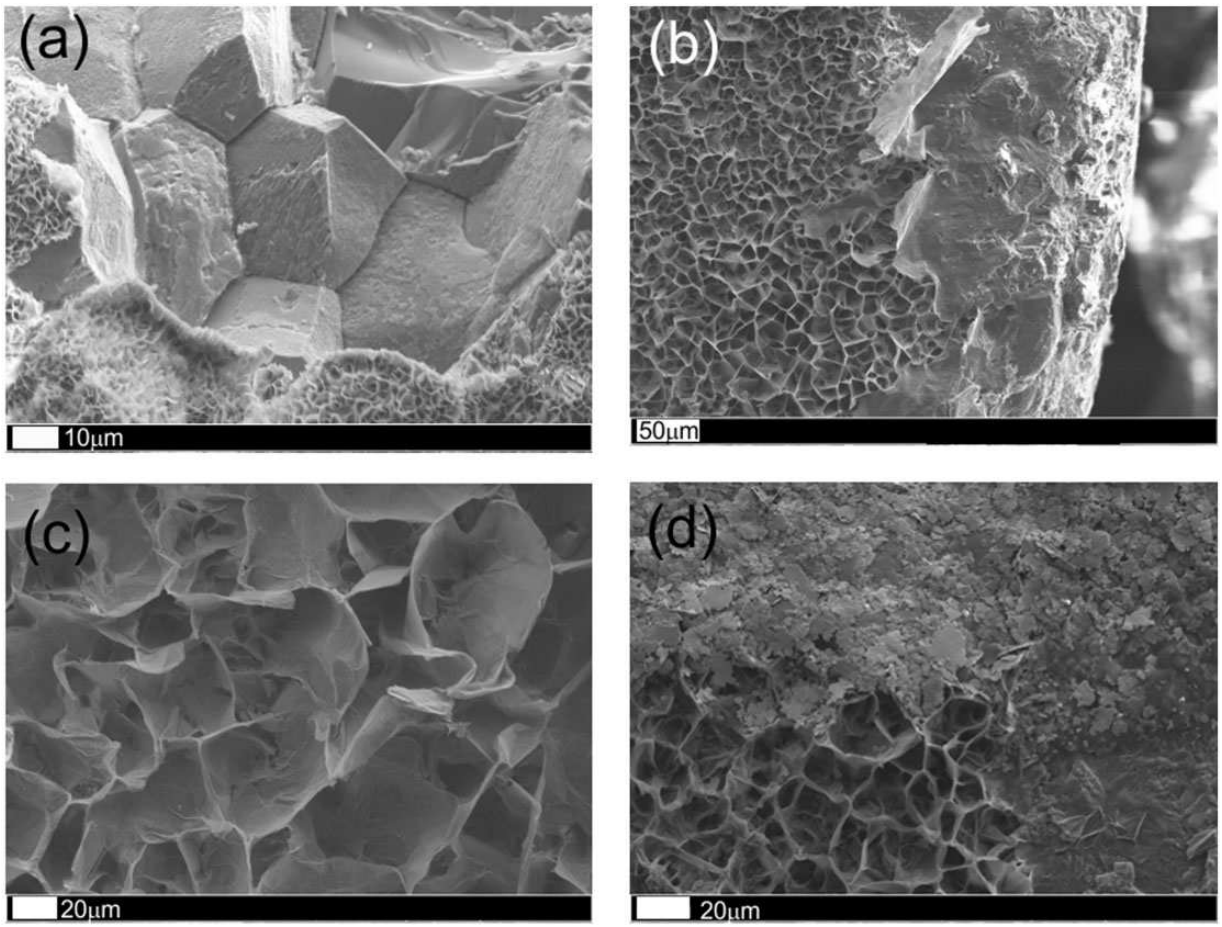

Fig. 4. SEM images of the outer surfaces of reacted cores of a natural basic hornfels to illustrate the effect of temperature on the grain size of saponite; all experiments were at 300 MPa and further details are given in Tables 2 and 4. (a) The interior hornfels texture is visible, and the outer coating of honeycomb saponite is particularly fine grained, capsule 52, 300°C; (b) intermediate saponite cells coat the surfaces and on the right are seen to be coated with a thin silica quench product, peeled off into a roll near the top of the image, capsule 37, 400°C; (c) detail of coarse saponite cells formed at 500°C, capsule 39; (d) honeycomb saponite partially blanketed by quench product, capsule 55, 400°C with 1M NaCl solution. [Note the similarity in the saponite cell size to capsule 37 (b) run at the same temperature without NaCl.]

the GFZ Potsdam, with a JEOL JXA 8500F field emission electron microprobe. The sample current was reduced to 10 nA to minimize damage during the analyses, which were carried out using a potential of 8 or 15 kV. In general a 1 μm spot size was needed because of the fine particle size, and we found no evidence of significant chemical variation in the course of an analysis. An example of a polished clump of enstatite and oligoclase grains held together by sheet silicates is shown in Fig. 5d. Although the bulk of the products are saponite, some intergrown talc is present and can be distinguished in the BSE image by its paler shade. In accordance with the complexity of the XRD patterns, it appears that single experiments can yield a range of phyllosilicates. Saponite is invariably present in runs with plagioclase, but shows considerable variation in composition, especially in Al content, within single samples. Talc is also present in all powder runs, except possibly some runs with powdered hornfels. The talc is invariably rather pure, and distinctly lower in Al than any saponites. Some runs also produced chlorite, although this appears to occur as a replacement of trace biotite.

Despite the obvious challenges in obtaining quantitative analyses from this sort of material, consistent trends do emerge. Saponites grown from enstatite–oligoclase mixtures not only have higher Mg/Fe than those grown from hornfels cores, reflecting the starting materials, they are also distinctly poorer in Al and richer in Si. Saponites from hornfels powder experiments have intermediate Al contents between saponite from enstatite–oligoclase mixtures and saponite produced from hornfels cores. In all cases, Al is predominantly in tetrahedral sites, although there is considerable analytical uncertainty in the site allocations. There are also consistent differences for all starting materials between experiments in pure water and those in

Downloaded from http://petrology.oxfordjournals.org/ at Edward Boyle Library on August 15, 2014

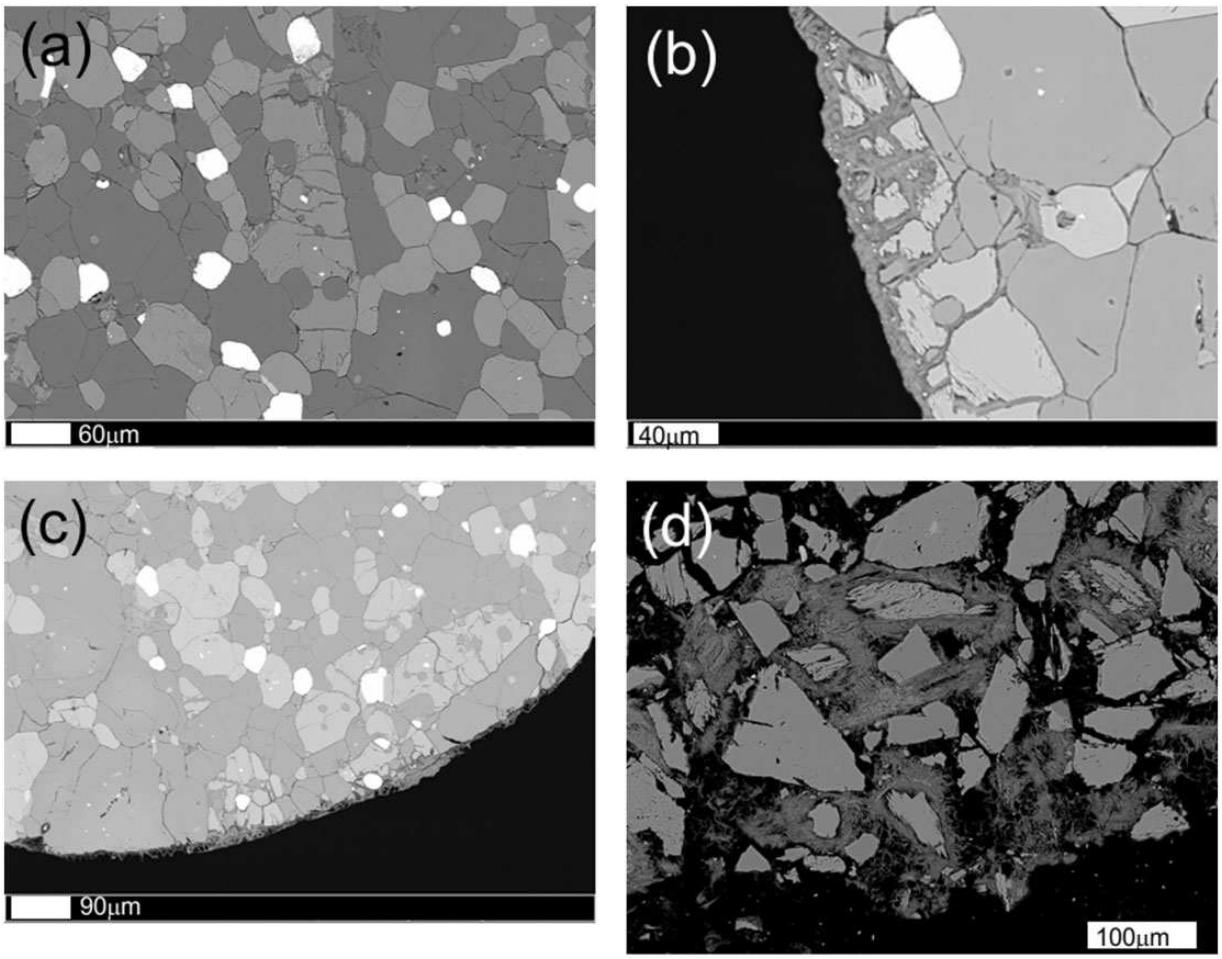

Fig. 5. BSE images of run products. (a)–(c) are all from a section of capsule 29 (Table 4) and show original magnetite (white), pyroxenes (pale grey) and plagioclase (dark grey). They also illustrate the minor amounts of original alteration (a) and the concentration of alteration on orthopyroxene grains exposed at the margins of the core (b, c). A large orthopyroxene grain inboard of the margin in (c) shows little more alteration than those in the interior (a). (d) is from powder sample 58 (Table 2) and illustrates the way in which secondary grains bind the original grains together; most of the secondary material is saponite but some paler talc is visible near the centre of the image (Table 5).

NaCl solutions: experiments in pure water yield Ca-saponite relatively rich in Al, whereas those grown in NaCl solutions have higher to dominant Na, according to salinity, and lower Al. Details of saponite compositions are given in Table 5 and summarized in Fig. 6.

There is little difference in chemical composition between saponites formed from hornfels cores under different P–T conditions. The large differences in grain size observed between saponite grown on hornfels cores at 300°C and 500°C (Fig. 4) are not reflected in any systematic chemical differences. It does appear, however, that the core experiments at 40 MPa, 400°C and at 300 MPa, 300°C have produced particularly Al-rich saponites, and indeed the 40 MPa sheet silicates appear to have an excess of octahedral cations and may be intermediate towards chlorite (Table 5). There are differences between saponites from the hornfels powder experiments and from the hornfels core experiments. The most Al-rich saponites are from core experiments with conditions of low P or low T, where we would expect the slowest rate of hydration, and hence least growth of saponite. This is of significance when it comes to balancing the reaction.

We can express the reaction whose rate has been measured from hydration of enstatite–oligoclase mixtures to a first approximation (based on the Ca content of saponite) as

$$0 \cdot 5\ CaAl_2Si_2O_8 + 8 \cdot 5\ MgSiO_3 + 3\ H_2O + 1 \cdot 75\ SiO_2 = Ca_{0\cdot5}Mg_{8\cdot5}AlSi_{11\cdot25}O_{30}(OH)_6$$

However, this reaction underestimates the Al content of the analysed saponites; they have a higher content of Al than can be derived from stoichiometric breakdown of plagioclase. For a typical saponite analysis from the enstatite–oligoclase mixes with around 0·45 atoms Ca per 33 O (Table 5) we would expect 0·9 atoms of Al from dissolution

Downloaded from http://petrology.oxfordjournals.org/ at Edward Boyle Library on August 15, 2014

Table 5: Analyses of saponite run products

	Hornfels cores															Hfels powder	Mineral powders			
Sample:	52	50	50	9	9	37	37	48	48	48	55	55	7	7	39	71	43	58	59	60
P (MPa)/*T* (°C)/M NaCl:	300/300	40/400	40/400	300/400	300/400	300/400	300/400	300/400	300/400	300/400	300/400/1M	300/400/1M	300/400/3M	300/400/3M	300/500	100/400	40/400	300/400/IM	300/400	300/400
Run time (h):	840	1176	1176	1848	1848	1368	1368	1368	1368	1368	672	672	1848	1848	672	672	1176	642	720	720
	Rim	Rim	Rpl	Inr Rim	Otr Rim	Rim	Rpl	Rim	Edge Rpl	Core Rpl	Rim	Rpl	Inr Rim	Otr Rim	Rim					
wt %																				
SiO_2	38·1	37·1	34·7	40·9	42·4	38·4	36·9	41·3	40·9	39·5	40·7	41·1	40·6	41·4	42·3	41·2	43·6	44·5	44·5	43·2
TiO_2	0·08	0·05	0·01			0·03	0·09	0·04	0·10	0·06	0·06	0·68			0·08	0·06	0·02	0·02	0·01	0·02
Al_2O_3	12·4	12·0	13·2	9·52	10·1	8·71	10·6	9·76	10·7	10·8	8·22	8·30	7·76	7·74	10·0	7·05	5·32	4·90	5·44	5·47
MgO	14·1	19·7	22·2	15·8	17·4	13·5	15·6	17·2	18·1	20·1	16·8	16·9	17·4	17·5	17·0	17·8	22·4	22·3	22·7	21·8
FeO	10·1	10·2	13·7	12·2	13·8	9·92	12·5	10·6	11·9	13·8	9·66	10·6	12·4	11·8	9·82	9·45	1·32	1·33	1·30	1·19
MnO	0·16	0·12	0·09			0·14	0·16	0·16	0·18	0·21	0·17	0·22			0·15	0·13	0·01	0·02	0·02	0·00
CaO	1·83	1·03	0·66	2·77	2·60	1·93	1·56	2·51	2·22	1·19	0·78	1·02	0·60	0·61	1·91	1·41	1·04	1·10	1·87	1·67
Na_2O	0·19	0·05	0·06	0·32	0·28	0·21	0·20	0·37	0·29	0·14	1·85	2·23	2·50	2·14	0·37	0·08	0·09	0·73	0·22	0·13
K_2O	0·13	0·13	0·06	0·19	0·12	0·11	0·24	0·10	0·14	0·10	0·28	0·47	0·21	0·08	0·14	0·04	0·06	0·21	0·08	0·08
BaO	0·09	0·09	0·03			0·06	0·04	0·10	0·07	0·12	0·10	0·07			0·06	0·14	0·10	0·08	0·10	0·11
Cl	0·53	0·02	0·00			0·05	0·03	0·03	0·02	0·01	0·49	0·88	0·04	0·02	0·02	0·04	0·06	0·30	0·03	0·04
Total	77·7	80·5	84·7	81·6	86·6	73·1	77·9	82·2	84·6	86·0	79·1	82·5	81·6	81·3	81·8	77·4	74·0	75·5	76·2	73·7
n	4	3	2	6	12	2	2	5	6	8	7	7	3	7	4	8	7	5	12	2
Cations to 33(O)																				
Si	9·67	9·09	8·28	9·94	9·77	10·29	9·46	9·90	9·59	9·22	10·17	9·99	9·96	10·10	10·08	10·35	10·87	10·96	10·81	10·83
Ti	0·015	0·009	0·002			0·006	0·017	0·007	0·017	0·010	0·011	0·122			0·014	0·011	0·004	0·003	0·003	0·005
Al	3·70	3·47	3·72	2·73	2·73	2·75	3·21	2·76	2·96	2·98	2·42	2·38	2·24	2·22	2·81	2·11	1·56	1·42	1·56	1·62
Mg	5·33	7·17	7·90	5·72	5·97	5·39	5·97	6·15	6·31	6·98	6·25	6·13	6·36	6·38	6·01	6·68	8·32	8·17	8·20	8·15
Fe	2·14	2·09	2·73	2·48	2·66	2·23	2·69	2·13	2·33	2·70	2·02	2·16	2·56	2·41	1·96	1·99	0·275	0·274	0·264	0·249
Mn	0·034	0·026	0·018			0·033	0·034	0·032	0·035	0·042	0·036	0·045			0·030	0·028	0·002	0·004	0·004	0·000
Ca	0·500	0·268	0·169	0·719	0·643	0·552	0·429	0·645	0·559	0·298	0·209	0·266	0·156	0·159	0·485	0·382	0·278	0·291	0·487	0·448
Na	0·092	0·022	0·027	0·157	0·128	0·109	0·100	0·173	0·130	0·064	0·902	1·053	1·218	1·012	0·176	0·041	0·042	0·342	0·102	0·065
K	0·041	0·039	0·019	0·063	0·035	0·038	0·077	0·031	0·042	0·029	0·088	0·147	0·067	0·026	0·043	0·013	0·018	0·067	0·024	0·026
Ba	0·008	0·009	0·003			0·006	0·004	0·009	0·007	0·011	0·010	0·006			0·005	0·014	0·010	0·008	0·009	0·011
Cl	0·243	0·010	0·001			0·023	0·012	0·012	0·009	0·003	0·208	0·360	0·017	0·010	0·008	0·016	0·026	0·123	0·012	0·017
Total	21·78	22·20	22·88	21·81	21·94	21·43	22·01	21·83	22·00	22·33	22·32	22·66	22·58	22·32	21·62	21·63	21·40	21·66	21·48	21·42

Additional details of runs are given in Tables 2 and 4. Inr, inner; Otr, outer; Rpl, replacement.

Downloaded from http://petrology.oxfordjournals.org/ at Edward Boyle Library on August 15, 2014

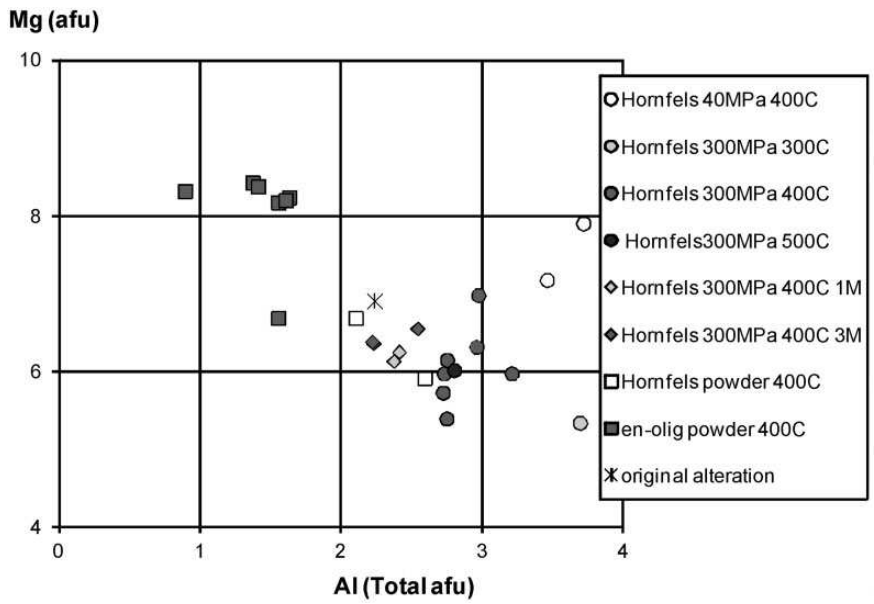

Fig. 6. Relationship between Mg and Al in synthetic saponites (Table 5). Oligoclase–enstatite powder experiments (Table 2) give very similar compositions irrespective of *P*–*T* conditions, and are rich in Mg, reflecting the starting materials (Table 1). Saponite from hornfels cores is distinct and has a greater spread in composition, with the most extreme compositions from experiments (Table 4) in which only small amounts of saponite were produced. It should be noted that hornfels powder experiments are intermediate between the two clusters of data, with a low Al content believed to reflect the extensive reaction.

of the anorthite component of feldspar, with a much smaller amount from albite dissolution. Actual levels of Al are over 1·5 times this. For saponites from core experiments, the discrepancies are even larger, especially for runs at 40 MPa, for which we predict relatively sluggish reaction. It is difficult to identify any solid phase that might have been present in the enstatite–oligoclase experiments and could have contributed additional Al or acted as a sink for Ca, although for the hornfels experiments it is possible that minor mineral components in the rock could have played a role. Given that the powder experiments with the most extensive reaction yield the highest Ca:Al ratios (i.e. are most nearly balanced), we consider it likely that the fluid acts as a reservoir for additional Ca (and Na) released from plagioclase breakdown, so that the reaction has the form

$$0 \cdot 75\ CaAl_2Si_2O_8 + 8 \cdot 5\ MgSiO_3 + 3 \cdot 25\ H_2O + 0 \cdot 875\ SiO_2 = Ca_{0\cdot5}Mg_{8\cdot5}Al_{1\cdot5}Si_{10\cdot875}O_{30}(OH)_6 + 0 \cdot 25\ Ca(OH)_2.$$

This reaction is possible only if the amount of water involved is large relative to the amount of mineral that reacts. In the crust, the large mass of rock relative to water will preclude reactions of this type, in which a significant amount of material can be removed into the fluid phase without any complementary exchange. It is in keeping with this reaction that the low-*P* hornfels cores that have produced the least saponite show the greatest discrepancy between Al and Ca concentrations in the saponite, assuming both elements are sourced from plagioclase. In contrast, the powder experiments in which reaction was most extensive have Al concentrations much closer to 2× those of Ca. This interpretation implies a relatively alkaline final fluid, for which we have no direct evidence beyond the observation that, after puncturing and drying the capsules, it was sometimes difficult to obtain a stable weight; this might have been the result of absorption of atmospheric CO_2. The Ca contents of fluids from core experiments in pure water implied by this reaction are of the order of tens to a few hundreds of parts per million, depending on the extent of reaction. Core experiments carried out with NaCl solutions yielded Na-saponites with much lower levels of Ca but only slightly lower Al than than those from pure water experiments. However, in these cases it is more reasonable to suppose that Ca was taken up into the fluid phase through the availability of Cl.

In summary, the hydration rates we have measured are for the reaction of enstatite to talc or enstatite plus plagioclase to a saponite clay that could be metastable under the conditions at which it grew. Detailed balancing of the reaction has proved difficult and it may be that components in the fluid phase were important.

DISCUSSION AND CONCLUSIONS

Relevance to natural reactions

Saponite, the major product of the hydration reactions described here, is a widespread alteration product of mafic

Downloaded from http://petrology.oxfordjournals.org/ at Edward Boyle Library on August 15, 2014

rocks in seafloor environments, but is not normally found in retrogressed rocks from deeper crustal settings. Whitney (1983) has demonstrated that different composition saponites formed metastably from gels will progressively recrystallize to more stable phases, including talc, chlorite, micas or other clays. Because our experiments probably did not produce the stable product for the P–T conditions, are the rates we have measured of relevance? Unlike prograde reactions, rates of retrograde reactions depend on interface reactions once water has been supplied, and will therefore be the same wherever water is added to an unstable anhydrous assemblage at a particular pressure and temperature, irrespective of the setting. We hypothesize that whenever water penetrates fractured rocks with orthopyroxene and plagioclase at temperatures up to 500°C the initial hydration product will be metastable saponite, but this will recrystallize to more stable phases over a time scale that is geologically rapid but slow by experimental standards. For example, the Al-rich saponite composition produced in the hornfels core experiments at low pressures has a composition intermediate between tremolite/actinolite and clinochlore-rich chlorite. Chlorite with intergrown needles of actinolite is a common texture in hydrothermally altered basalts, and occurs in veins cutting the outcrops of hornfels from which our sample was collected. Our results suggest that such intergrowth textures may arise from recrystallization of an original metastable saponite, rather than directly from precursor high-T phases.

Significance for crustal rheology

It is evident that substantial amounts of hydration can occur in the middle crust over a time scale of months with starting assemblages including orthopyroxene, or kyanite + biotite. To put these observations into the context of retrograde fluid infiltration into crystalline crust, and hence determine whether crystalline crust is likely to remain wet for long periods of time after water infiltrates, we must make assumptions about how water enters the crust. Clearly, for water to reach regions of the mid to lower crust where they are composed of potentially reactive lithologies, the initial flow rate must be rather rapid. From the distribution of retrograde alteration in crystalline rocks it is reasonable to assume that water infiltrates along networks of cracks, but for simplicity we will consider one crack. The thickness of the water film present in the crack initially is an unknown, but by comparison with secondary fluid inclusions in vein quartz formed under comparable conditions, which have dimensions typically in the 5–10 μm range, it seems reasonable to assume that the water film is significantly thicker than this, and so we have assumed a value of 200 μm. The data presented in Fig. 3 can then be used to calculate how long it will take for a 100 μm water film to be absorbed onto 1 m^2 of fracture surface; that is, the time taken to consume each half thickness of the water film on the adjacent fracture wall. We have also assumed that the natural fracture roughness is the same as the roughness factor assumed for grains in the powder experiments.

Figure 7 shows the calculated times for this standard water film to be consumed, from both the data reported here (Table 2, Fig. 3) and the earlier published work of Schramke *et al.* (1986) and Yardley *et al.* (2010). The results plotted indicate that the water will be consumed over a comparable time scale by a range of wall-rocks, including pelites, orthopyroxene-bearing rocks and basic granulites. This represents a wide range of the relatively reactive rock types commonly present in the continental crust. Most data are available for 400°C, but it appears that the effects of temperature on reaction rate are not large. The overwhelming majority of the experimental data indicate that the maximum length of time for which a film of free water can remain in the model crack system is of the order of a few tens of years to 100 years. Data points indicating shorter residence times are included in Fig. 7a, but are from experiments that were identified earlier as yielding overestimates of the amount of water reacted. When the outliers are removed in Fig. 7b, it is clear that the spread in results is across almost an order of magnitude, with a strong concentration of the new data around 20 years for the persistence of the model water film. Although the uncertainties are large, the results all indicate very rapid hydration and a short residence time for water in crystalline crust under conditions where retrogression is possible, and it seems clear that water cannot normally be resident in cooled crystalline crust at mid to lower crustal depths. The use of water-saturated rheologies for the deep crust of plate interiors in geodynamic models is therefore not appropriate.

It remains true that water-mediated deformation mechanisms are extremely important in the crust, but our results show that they can develop only during prograde dehydration, when free water is ubiquitous, or in response to specific infiltration events affecting cooled crystalline rocks. If unreacted high-grade relict assemblages are still present, free water will be consumed rather rapidly and must be replenished to permit deformation to continue.

The production of clay minerals during retrograde alteration must, of course, influence rock strength, and crystalline rocks cut by clay-lined veins are likely to be weaker than the pristine precursor. Nevertheless, even when clays are present, additional pressure solution processes are needed to greatly reduce rock strength (Bos & Spiers, 2002) and our results show that, until the fault rocks are fully hydrated, this can happen only intermittently. Recent results from the SAFOD drilling project demonstrate the importance of pressure solution for deformation even in the weak fault gouge that was encountered (Holdsworth *et al.*, 2011). Interestingly, if, as we suggest,

Downloaded from http://petrology.oxfordjournals.org/ at Edward Boyle Library on August 15, 2014

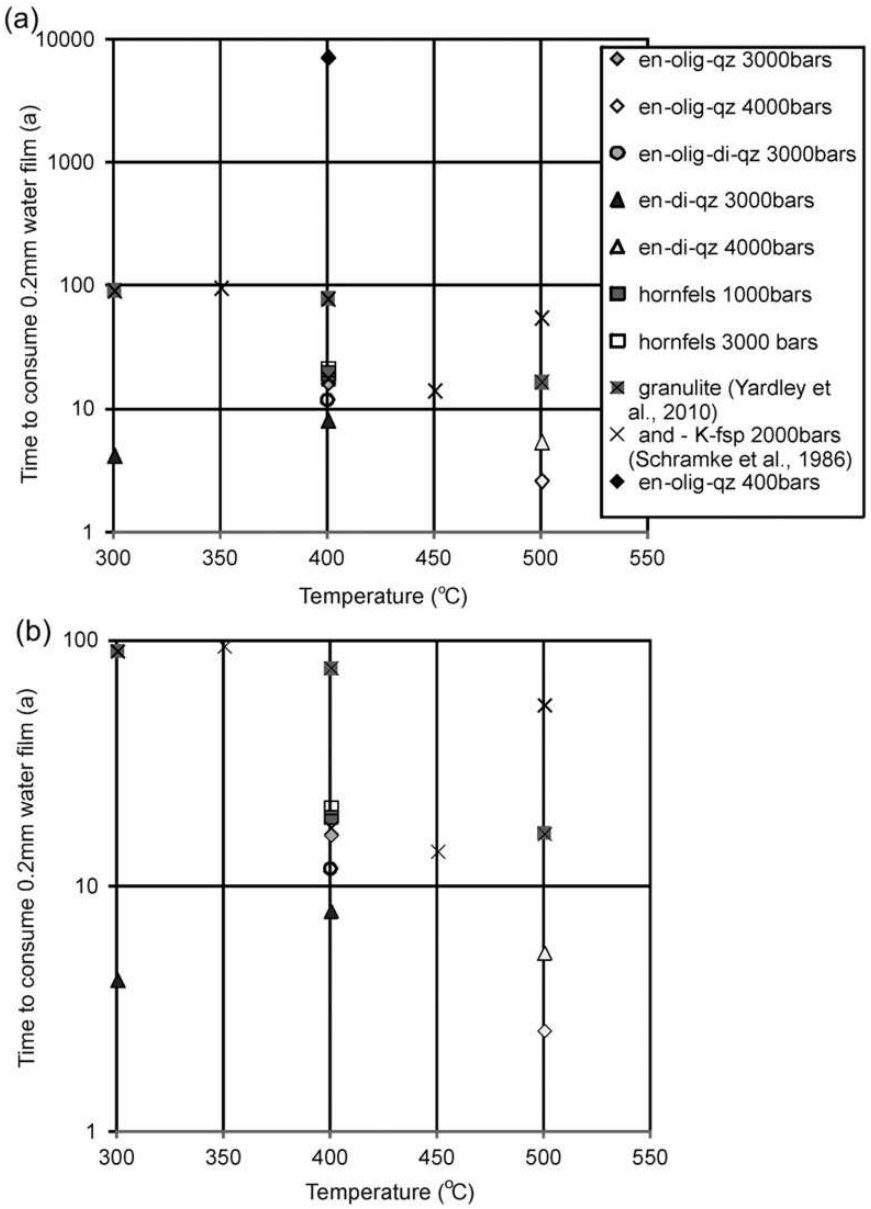

Fig. 7. (a) Synthesis of all available experimental data, calculated to show the time taken to consume a 100 μm thick half film of water by hydrating a crack wall. With the exception of one data point at low pressure, all the data suggest that such a film will be consumed in less than 100 years, with only a minor effect of temperature in the mid to lower crustal range investigated. (b) The same dataset with likely outliers removed to show the strong concentration of results around a hydration time of a few tens of years.

water is often not present continuously, healing of fault rocks will be inhibited so that they remain longer as planes of weakness (Bos & Spiers, 2000).

One final point for consideration is the role of water flow. The discussion thus far has mainly focused on a scenario of small amounts of water penetrating along cracks to produce local retrogression of the walls. Such retrograded rocks often show some evidence for metasomatic modification of composition by fluid infiltration (e.g. Zack *et al.*, 2001; Holness, 2003), and this implies significantly larger quantities of water than we have considered in the end-member model presented here, in which water infiltrates a fracture and remains in place until consumed. Retrogression is often accompanied by localized deformation and most shear zones show evidence for metasomatism, extensive retrogression and coupling of fluid flow with deformation. Mancktelow & Pannacchioni (2005) have demonstrated how mid-crustal shear zones may initiate as brittle features but become ductile shears as water penetrates. The development of phyllosilicates along

Downloaded from http://petrology.oxfordjournals.org/ at Edward Boyle Library on August 15, 2014

discrete shears in a crystalline rock results in permanent weakening so that existing shears focus further deformation (Raimondo *et al.*, 2011; Goncalves *et al.*, 2012). The same calculations of water consumption still apply in the mobile case, although they only indicate the time for water to be consumed after flow ceases. Hence retrograded fractures might have remained open and wet for longer periods of time than these calculations indicate, but the additional time for which they remained wet is constrained by the requirement for a continuous source of water. Only when the primary shear zone assemblage is fully hydrated can free water remain indefinitely. Because major earthquakes repeat on time scales of several hundred years, it is likely that even active shear zones remain dry for much of the time. Irrespective of the presence of a water phase, phyllosilicate-rich rocks provide continuing zones of weakness in crystalline host-rocks (Holdsworth *et al.*, 2001; van Diggelen *et al.*, 2010).

In summary, the results presented here demonstrate that many crystalline rocks of the mid to lower crust react with water so rapidly that the extent of retrograde hydration is limited by the extent to which water is able to penetrate. The widespread survival of high-grade rocks in the crust through geological time is a testament to the dry nature of most of the continental crust for most of the time. Even within deformation zones where water can be periodically replenished, for example by seismic events, the reaction rate is likely to be sufficiently fast for all water to be consumed between successive reinjections. Only once wall-rocks around fluid-filled fractures have been fully hydrated can water remain for extended periods. These results make it clear that, even within zones of active deformation, crystalline rocks in the mid to lower crust that have cooled below their original formation temperature will almost invariably be dry, in the sense that they will not contain a free water phase. At sites where fractures have allowed ingress of water from the upper crust, water can survive for periods of tens to perhaps a few hundreds of years before it has been completely consumed by hydration reactions, and at these sites significant water weakening may occur, but it will be restricted to the narrow zone of water infiltration and will be transient in nature. At other times, crustal rheology will be dictated by dry rocks containing zones with fractures and fine-grained hydrous minerals.

ACKNOWLEDGEMENTS

We are indebted to Dan Harlov, Bernd Wunder, Reiner Schulz and Hans-Pieter Nabein for advice and help with the experimental techniques, and to Dan Harlov and Ralf-Thomas Schmitt of the Museum für Naturkunde, Berlin, for the provision of mineral samples. SEM observations were made with the help of Dr H. Kemnitz and Dan Harlov at the GFZ, with additional work in Leeds assisted by Eric Condliffe. An earlier draft was greatly improved by the comments of Toru Takeshita and an anonymous reviewer.

FUNDING

This work was supported by the Alexander von Humboldt Foundation through a Humboldt Award to BWDY, and by the Helmholtz Centre Potsdam.

REFERENCES

Allan, M. M., Turner, A. & Yardley, B. W. D. (2011). Relation between the dissolution rates of single minerals and reservoir rocks in acidified pore waters. *Applied Geochemistry* **26**, 1289–1301.

Billings, M. P. (1937). Regional metamorphism of the Littleton–Moosilauke area, New Hampshire. *Geological Society of America Bulletin* **50**, 181–238.

Blanpied, M. L., Marone, C. J., Lockner, D. A., Byerlee, J. D. & King, D. P. (1998). Quantitative measure of the variation in fault rheology due to fluid–rock interactions. *Journal of Geophysical Research* **103**, 9691–9712.

Bos, B. & Spiers, C. J. (2000). Effect of phyllosilicates on fluid-assisted healing of gouge-bearing faults. *Earth and Planetary Science Letters* **184**, 199–210.

Bos, B. & Spiers, C. J. (2002). Frictional–viscous flow of phyllosilicate-bearing fault rock: microphysical model and implications for crustal strength profiles. *Journal of Geophysical Research* **107**, doi:10.1029/2001JB000301.

Burov, E. B. (2011). Rheology and strength of the lithosphere. *Marine and Petroleum Geology* **28**, 1402–1443.

Ferry, J. M., Mutti, L. J. & Zuccala, G. J. (1987). Contact-metamorphism hydrothermal alteration of Tertiary basalts from the Isle of Skye, northwest Scotland. *Contributions to Mineralogy and Petrology* **95**, 166–181.

Goncalves, P., Oliot, E., Marquer, D. & Connolly, J. A. D. (2012). Role of chemical processes on shear zone formation: an example from the Grimsel metagranodiorite (Aar massif, Central Alps). *Journal of Metamorphic Geology* **30**, 703–722.

Holdsworth, R. R., Stewart, M., Imber, J. & Strachan, R. A. (2001). The structure and rheological evolution of reactivated continental fault zones: a review and case study. In: Miller, J. A., Holdsworth, R. E., Buick, I. S. & Handy, M. R. (eds) *Continental Reactivation and Reworking. Geological Society, London, Special Publications* **184**, 115–137.

Holdsworth, R. E., van Diggelen, E. W. E., Soiers, C. J., de Bresser, J. H. P., Walker, R. J. & Bowen, L. (2011). Fault rocks from the SAFOD core samples: implications for weakening at shallow depths along the San Andreas Fault, California. *Journal of Structural Geology* **33**, 132–144.

Holness, M. B. (2003). Growth and albitization of K-feldspar in crystalline rocks in the shallow crust: a tracer for fluid circulation during exhumation? *Geofluids* **3**, 89–102.

Kenis, I., Urai, J. L., van der Zee, W., Hilgers, C. & Sintubin, M. (2005). Rheology of fine-grained siliciclastic rocks in the middle crust—evidence from structural and numerical analysis. *Earth and Planetary Science Letters* **233**, 351–360.

Knauss, K. G., Nguyen, S. N. & Weed, H. C. (1993). Diopside dissolution kinetics as a function of pH, CO_2, temperature and time. *Geochimica et Cosmochimica Acta* **57**, 285–294.

Downloaded from http://petrology.oxfordjournals.org/ at Edward Boyle Library on August 15, 2014

Kohlstedt, D. L., Evans, B. & Mackwell, S. J. (1995). Strength of the lithosphere: constraints imposed by laboratory experiments. *Journal of Geophysical Research* **100**, 17587–17602.

Mancktelow, N. & Pennacchioni, G. (2005). The control of precursor brittle fracture and fluid–rock interaction on the development of single and paired ductile shear zones. *Journal of Structural Geology* **27**, 645–661.

Oelkers, E. H. & Schott, J. (1995). Experimental study of anorthite dissolution and the relative mechanism of feldspar hydrolysis. *Geochimica et Cosmochimica Acta* **59**, 5039–5053.

Oelkers, E. H. & Schott, J. (2001). An experimental study of enstatite dissolution rates as a function of pH, temperature and aqueous Mg and Si concentration, and the mechanism of pyroxene/pyroxenoid dissolution. *Geochimica et Cosmochimica Acta* **65**, 1219–1231.

Raimondo, T., Clark, C., Hand, M. & Faure, K. (2011). Assessing the geochemical and tectonic impacts of fluid–rock interaction in mid-crustal shear zones: a case study from the intracontinental Alice Springs Orogen, central Australia. *Journal of Metamorphic Geology* **29**, 821–850.

Rutter, E. H. (1983). Pressure solution in nature, theory and experiment. *Journal of the Geological Society, London* **140**, 725–740.

Schramke, J. A., Kerrick, D. M. & Lasaga, A. C. (1986). The reaction muscovite + quartz = andalusite + K-feldspar + water; Part 1, growth kinetics and mechanism. *American Journal of Science* **287**, 517–559.

Schwartz, G. M. & Todd, J. H. (1941). Comments on retrograde metamorphism. *Journal of Geology* **49**, 177–189.

Seyfried, W. E. & Bischoff, J. L. (1979). Low temperature basalt alteration by seawater: an experimental study at 70°C and 150°C. *Geochimica et Cosmochimica Acta* **43**, 1937–1947.

Turner, F. J. (1968). *Metamorphic Petrology—Mineralogical, Field and Tectonic Aspects*, 2nd edn. New York: McGraw–Hill.

Van Diggelen, E. W. E., De Bresser, J. H. P., Peach, C. J. & Spiers, C. J. (2010). High shear strain behaviour of synthetic muscovite fault gouges under hydrothermal conditions. *Journal of Structural Geology* **32**, 1685–1700.

Whitney, G. (1983). Hydrothermal reactivity of saponite. *Clays and Clay Minerals* **31**, 1–8.

Yardley, B. W. D. (2009). The role of water in the evolution of the continental crust. *Journal of the Geological Society, London* **166**, 585–600.

Yardley, B. W. D., Mackenzie, W. S. & Guildford, C. (1990). *Atlas of Metamorphic Rocks and their Textures*. Longman.

Yardley, B. W. D., Harlow, D. E. & Heinrich, W. (2010). Rates of retrograde metamorphism and their implications for crustal rheology. *Geofluids* **10**, 234–240.

Zack, T., Rivers, T. & Foley, S. F. (2001). Cs–Rb–Ba systematics in phengite and amphibole: an assessment of fluid mobility at 2·0 GPa in eclogites from Trescolmen, Central Alps. *Contributions to Mineralogy and Petrology* **140**, 651–669.

Downloaded from http://petrology.oxfordjournals.org/ at Edward Boyle Library on August 15, 2014